A Method Estimating Plug’s Power Usage Pattern for Public Electric Vehicle Charging Stations within Multi-Uncertainty Parameters in Indonesia Urban Area

Kurniasari, Asih
Intelligent Power Energy System (InPES), Research Center for Energy Conversion and Conservation

Abdul Wachid Syamroni
Intelligent Power Energy System (InPES), Research Center for Energy Conversion and Conservation

Moch Arief Albachrony
Intelligent Power Energy System (InPES), Research Center for Energy Conversion and Conservation

Galih Prasetya Dinanta
Research Center for Remote Sensing National Research & Innovation Agency (BRIN)

他

https://doi.org/10.5109/7151744

出版情報：Evergreen. 10 (3), pp.1904-1915, 2023-09. 九州大学グリーンテクノロジー研究教育センター
バージョン：

A Method Estimating Plug's Power Usage Pattern for Public Electric Vehicle Charging Stations within Multi-Uncertainty Parameters in Indonesia Urban Area

Asih Kurniasari[1,*], Abdul Wachid Syamroni[1], Moch Arief Albachrony[1], Galih Prasetya Dinanta[2], Danang Yogisworo[1], Tisha A.A.Jamaluddin[1], Abdul Aziz Basharah[1], Cuk Supriyadi Ali Nandar[1]
[1]Intelligent Power Energy System (InPES), Research Center for Energy Conversion and Conservation
[2]Research Center for Remote Sensing National Research & Innovation Agency (BRIN), Indonesia

*Author to whom correspondence should be addressed:
E-mail: asih.kurniasari@brin.go.id

(Received April 30, 2023; Revised July 18, 2023; accepted July 26, 2023).

Abstract: The uncertainty parameters driven by diverse user behavior, battery types, and charger instruments of electric mobility (e-mobility) would pose risk challenges to existing grid assets' adequacy and reliability issues. Using the pseudorandom of the Monte Carlo method, this research constructs an estimation framework to generate power intake of public electric vehicle charging stations (EVCSs) for a typical 20kV|0.4kV distribution grid urban area. This study suggested that those multi-uncertainties potentially threaten daily operations with a significant impact in low voltage grids with voltage magnitude dropping to 0.884 p.u. Nevertheless, recognizing and alerting to the future-changing and performance-preserving electric grid infrastructure should raise awareness as gradual employment is outpacing the national target of the energy transition.

Keywords: uncertainty parameters; estimation power intake; electric vehicle charging station; Monte Carlo method; urban area; energy transition

1. Introduction

Modifying internal combustion engines (ICE), which release 167g of CO2 gas per kilometer, is one example of many initiatives to lower CO2 emissions and drastically reduce fuel usage, which is crucial to meeting the world's growing demand for energy. Although much progress has been made, there are still many gaps to fill in terms of ecological harm[1,2)]. Shifting vehicles from ICEs to electric vehicles (EVs) is one option targeting net zero emissions (NZE) since the transportation sector's overall carbon footprint could potentially increase as carbon emissions rise concurrently. Hence, these manifold carbon footprints could release other gases that worsen air pollution in the case of refrigerated vehicles[2,3)]. Another consideration is that it may increase the social environment and standard of living since EVs can make up to 22.7% less noise than standard ICE, i.e., motorcycles, which is suitable for urban city road[4,5)].

The shifting scenario reported by Energy International Agency (EIA) is that there will be over 350 million EVs in the NZE view[6)]. Many developed countries, including China, the United States (USA), and Canada, aim to end ICE production and sales by 2035. Even earlier, some European countries will not begin selling any autos except EVs until 2030[7–9)]. One of the critical successes of this acceleration in increasing the EV number and encouraging the owners to shift is the extensive infrastructure development of the so-called EVCS. As of record in the USA, the total EVCS reached 46,290 units with total plugs of 113,600 listed in early 2021, with the majority being allocated in public, i.e., the travel spots, conventional shops, restaurants, visitor points, and inter-city highways[10)]. While in Europe, the number of public charging points reached 224,237 units in 2020, with the Netherlands having the most charging points, rolled out by 64,000 regular chargers and 2500 fast chargers. Those accounted for one-half of the public charging point (PCP) ratio employed[11)]. These schemes are also undergoing in Southeast Asia, where Thailand is targeting 100% of EVs by 2035; the country has 664 EVCS units with a total plug of 2,224 units listed in June 2021[12)]. Indonesia has set an ambitious target through the Ministry of energy and mineral resources in the national grand energy strategy (GSEN), which currently has 219 units in 2021 (servicing out of 1760 four-wheeler EVs (4-Ws) existing units), reaching 695 units in this year's target (2022), to expected of 31,859 EVCS units servicing out of 2.19 million 4-Ws and also 13 million of two-wheelers EVs (2-Ws) by 2030[13)].

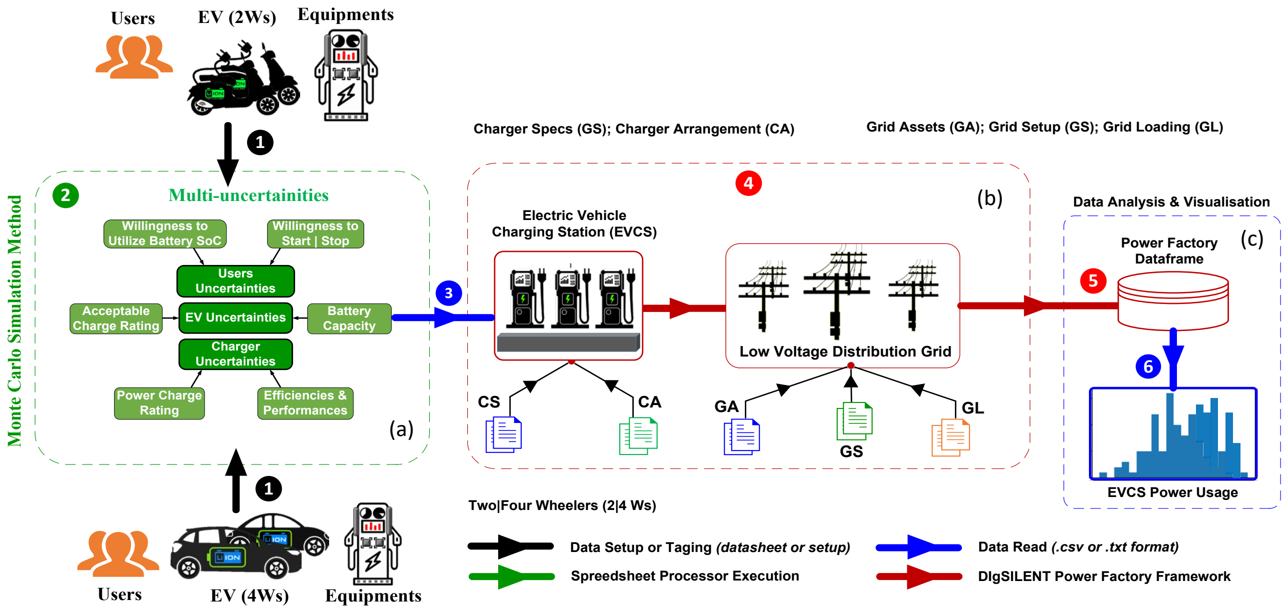

Fig 1: Sequential method of the research: (a) The proposed multi-uncertainties of the Monte-Carlo Simulation Method (MCSM), (b) Validation framework setup through PSA, (c) Data analysis and visualization

The planning of massive deployment of EVCS infrastructure is one of the most challenging tasks due to the complexity of EV and its derivative uncertainty in aligning the gradual phase of EV transformative adoption, which the grid utility must consider. The well-planned allocation and the quantity number of EVCS deployments, projection of the future regular load and EV demand to the grid's existing capacity, and the availability of funds for physical upgrading should be optimally and efficiently matched. Particularly in developing countries where the grid infrastructure assets are likely nearing the end of life expectancy, spare sizing-constrained, built-in frailty topology, and regulated structure in the non-competitive scheme[9,10,14]. Additionally, numerous EV variables emerge as uncertainties that are decisive to predict due to the interactional characteristics of the three combined parameters: the EV unit, the charger equipment, and the EV user behavior. Hence, these continuously caused uncertain conditions of related parameters, such as the occurring timeframe of starting/stopping the charging, the time duration from one to another session, and the amount of power intake during the charging progress[15].

Another consideration that would likely happen in the early phase of shifting from ICE to EV is the addicted manner of fueling different types of vehicles, so-called 'uncontrolled' mode charging based on user needs and preferences only at any time and place, which could happen in a residential or commercial in either urban or rural area. As a consequence, these may produce abrupt load pattern charging characteristics and impact the overall load profile, particularly in the feeder to which the EVCS is linked[16,17]. In most cases, it affects the voltage stability, stresses the thermal asset capacity, and jeopardizes the loading factor[18]. Consequently, the conventional grid topology is prone to those, leading to substantial system losses, power failure, outage, and likely impairment of electronic equipment[19]. Furthermore, if the grid asset's capacity does not match in a certain condition and repeats randomly, thus, results in economic and opportunity disadvantages from a broadened perspective.

For that reason, estimating usage patterns is essential during the deployment planning process in projecting changes and recognizing the impacts of e-mobility in the view of grid future-changing and performance-preserving. Besides, forecasting the potential revenues and initiating new business models obtained during the EVCS deployment from the beginning of the planning process increases the chances of a smooth transition[20]. At once, it enables the rethinking idea of utilizing local reserve and deferring the installation of new physical capacity, thus reducing the need for substantial in-front capital expenses while still retaining overall service quality as mandatory.

In this article, the multi-uncertainties that arose from the charging process, which includes each plug of two and four-wheelers (2|4-Ws) EVCS estimating the power intake fluctuation, have not yet been discussed or publicly available. Further, notable literature values that align with this research purpose are found in[6,7,17,18,20]. Despite those facts, our paper fills the critical gap in the literature by which considering the unknown entities (i.e., the timeframe of occurrence and the sense of user conducts and preferences) with the high possibility of diversities combining (i.e., technical specifications of EVs and supportive peripherals) but still in logically and reasonable sense. Also, our study investigates and tackles two tasks aligning the ongoing climate change mitigation and carbon regulations that may be strictly authorized in the upcoming days, as follows:

- The creation of a projection framework enables validation of the adequacy and security awareness of the existing distributed grid feeders (DGF) in terms of multi-uncertainties parameters that emerge from the charging process of public EVCS.

- Fostering sustainability (to get a proper solution in the transformative energy sector) by developing a practical validation framework based on the typical DGF in Indonesia's urban area within a reasonable time-varying execution representing the virtual model of DGF to which the deployment of supporting e-mobility infrastructure is deployed and operated.

2. Methodology

In general, the research methodology can be seen in Fig.1. It consists of three sequential execution platforms. The first platform (a) consists of two parts of workflows. Part 1 gathered information to create boundaries state by using all relevant data (primary or secondary), such as occupational behavior or working place in a particular area and existing public transportation, also EVs' and EVCSs' related products (stock market/sales, specs, and pricing, as well as new products potentially to be launched) from available public data repositories[21,22]. Next, Part 2 is the data collection and clustering process aligned with research aims, objectives, and requirements. Henceforth, two related sub-uncertainty parameters are retrieved from each; namely, the user's uncertainty constitutes the willingness to utilize the state of charge (SoC) of its battery capacity (UB_{SoC}^{U}) and the willingness to start or stop the charging process neglecting the SoC value $(UB_{S|S}^{U})$. Likewise, the EV's uncertainty consists of an acceptable charge rating (EV_{AR}^{U}) and the battery pack capacity(EV_{BC}^{U}). Lastly, the charger's uncertainty appoints to the power charges rating (CH_{PR}^{U}) and chargers' efficiency and performance (CH_{EP}^{U}). Hence, deriving the proposed multi-uncertainties factors to generate the power usage pattern of the charging process for each plug using the statistical randomness of the Monte-Carlo simulation method (MCSM) modified from[23], by applying seed boundaries of minimum and maximum {min|max} values of each of those factors.

Part 3 is the data tagging process according to the data result in Part 2 through the soft-coupled method in the csv, txt, or json file format to align the acceptable data to be computed in the following process. In Part 4, as part of platform (b), the investigation and validation process through power system analysis (PSA) is carried out. It is expected to enable grid planners, operators, stakeholders, or policymakers to recognize the impact of uncertainties related to the existing infrastructure, including apparatus assets, grid operational setup, as well as regular customer loading in a virtual model of DGF by computing in dynamic time series power flows execution. The last workflow is defined in the platform (c), consists of Part 5 and Part 6 for data analysis and visualization, in which Part 5 emphasizes the process of storing result data in the internal data repository before being recollected and used to foresee the upcoming potential threads as of the topic discussion is done in Part 6.

2.1 User uncertainties

User uncertainties (UU) are the randomness influenced by EV's user behavior in the progress of the charging session and become one of the sturdy factors due to the unknown status of future-event either in active or idle mode. It is noticed that there are two different usage patterns strongly related to EV's user side. Firstly, the willingness of the EV's owners to begin (active mode of charging, T_{ON}^{Plug}) or stop (idle mode of charging, T_{OFF}^{Plug}) in any circumstances and time of occurrence. The UU is derived using the following criteria in Eq. 1 and Eq. 2. These conditions are influenced by the user's action, neglecting the range of its SoC capacity. To this end, we define the total hour of EVCS operation HO_{EVCS}^{active} is set for 1440 minutes, starting T_{EVCS}^{Set-ON} from 00:00 until $T_{EVCS}^{Set-OFF}$ at 24:00. Hence, the maximum plug's active duration T_{ON}^{Plug} is set for 100 minutes, and the minimum plug's idle duration T_{OFF}^{Plug} is set for 5 minutes.

$$UB_{S|S}^{U\,(2|4\,Ws)} \begin{cases} \xrightarrow{set} T_{EVCS}^{Set-ON} \leq HO_{EVCS}^{active} \leq T_{EVCS}^{Set-OFF} \\ HO_{EVCS}^{active} = \sum_{T_{EVCS}^{Set-ON}}^{T_{EVCS}^{Set-OFF}} \{T_{OFF}^{Plug}, T_{ON}^{Plug}\} = 1440 \\ \text{s.t.} \\ \xrightarrow{when} HO_{EVCS}^{active} \xrightarrow{If} Rand(T) = 1 \xrightarrow{then} \\ T_{ON}^{Plug}\,(1) \leq set\, T_{ON}^{Plug}(\text{2Ws|4Ws}) \\ \xrightarrow{when} HO_{EVCS}^{active} \xrightarrow{If} Rand(T) = 0 \xrightarrow{then} \\ T_{OFF}^{Plug}\,(0) \leq \text{5 minutes} \end{cases} \quad (1)$$

$$UB_{SoC}^{U\,(2|4\,Ws)} \begin{cases} \xrightarrow{set} SoC_{EV}^{Set-ON} \leq SoC_{EV}^{Rat} \leq SoC_{EV}^{Set-OFF} \\ SoC_{EVCS}^{Rat} = \sum_{SoC_{EV}^{Set-OFF}}^{SoC_{EV}^{Set-ON}} \{T_{OFF}^{Plug}, T_{ON}^{Plug}\} \\ \text{s.t.} \\ \xrightarrow{when} T_{ON}^{Plug} \xrightarrow{If} Rand(T) = 1 \xrightarrow{then} \\ SoC_{EV}^{Set-ON}\,(1) \geq 0.20 \\ \xrightarrow{when} T_{OFF}^{Plug} \xrightarrow{If} Rand(T) = 0 \xrightarrow{then} \\ SoC_{EV}^{Set-OFF}\,(0) \leq 0.85 \end{cases} \quad (2)$$

Secondly, the willingness of the EV user to utilize the battery based on its SoC value as their reference to start (SoC_{EV}^{Set-ON}) or stop the charging session $(SoC_{EV}^{Set-OFF})$ of which this condition is the opposite of the Eq. 1. Here in Eq. 2, SoC_{EV}^{Set-ON} is set at a minimum of 20% and $SoC_{EV}^{Set-OFF}$ at 85% of the SoC rating SoC_{EVCS}^{Rat} at 100%. The reference setting for this SoC value is based on Tesla user feedback about the ideal minimum and maximum SOC value concerning battery degradation of lithium batteries over the years of usage[24].

2.2 EV uncertainties

EV uncertainties (EVU) are a level of uncertainty defined by the acceptable charge rating EV_{AR}^{U} and battery capacity. The acceptable charge rating defines the current charging that the EV battery and its internal supporting devices safely operate. Here, the uncertainty EV_{AR}^{U} is set to have a maximum of 50% and a minimum of 99% of its power charges rating (CH_{PR}^{U}). While the battery rating capacity EV_{BC}^{U} is the maximum battery capacity of the EV unit that can be utilized in total[25]. The EVU is derived using the following criteria in Eq. 3 and Eq. 4.

In most cases, battery makers determine EV_{AR}^{U} to ensure a long battery lifespan. The new battery has an acceptable charge of 100% of its rating, whereas utilized batteries have never reached their initial rating over the years due to the charge cycle operation and aging. This capacity loss is called battery degradation and is scaled as depth of discharge (DoD). The average guarantee of DoD by automakers is found to be 80% after five to eight years of usage[26]. Here, the uncertainty of DoD (DoD^{U}) is set maximum of 80% and minimum 99%.

Table 1. The typical battery capacity of EV's brand in Indonesia.

EV 4-Ws	Battery capacity (kWh)	EV 2-Ws	Battery capacity (kWh)
Mitsubishi-Miev	16	Gesit	1.44
BMW	21.6	Volta	1.5
BYD	71.6	Winfly	1.44
Tesla	75	Viar	2
Nissan	40	United motor	1.6
Hyundai	40	Gesit	1.44

$$EV_{AR}^{U}(2|4\,Ws)\begin{cases}\xrightarrow{set\ (2|4\ \mathrm{Ws})} 0.5 * CH_{PR}^{U} \le EV_{AR}^{U} \le 0.99 * CH_{PR}^{U} \\ \text{s.t.} \\ \xrightarrow{when} T_{ON}^{Plug} \xrightarrow{If} Rand(T) = 1 \xrightarrow{then} \\ EV_{AR}^{U}(1) = (\rightarrow set\ (2|4\ \mathrm{Ws})) \\ \xrightarrow{when} T_{OFF}^{Plug} \xrightarrow{If} Rand(T) = 0 \xrightarrow{then} \\ EV_{AR}^{U}(0) = 0.00\end{cases} \quad (3)$$

$$EV_{BC}^{U}(2|4\,Ws)\begin{cases}\xrightarrow{set\ (2\ \mathrm{Ws})} 1.0\ \mathrm{kWh} \le EV_{BC}^{U} 3.4\ \mathrm{kWh} \\ \xrightarrow{set\ (4\ \mathrm{Ws})} 16\ \mathrm{kWh} \le EV_{BC}^{U} \le 75\ \mathrm{kWh} \\ \text{s.t.} \\ \xrightarrow{when} T_{ON}^{Plug} \xrightarrow{If} Rand(T) = 1 \xrightarrow{then} \\ EV_{BC}^{U}(1) = (\rightarrow set\ (2|4\ \mathrm{Ws}) * DoD^{U}) \\ \xrightarrow{when} T_{OFF}^{Plug} \xrightarrow{If} Rand(T) = 0 \xrightarrow{then} \\ EV_{BC}^{U}(0) = 0.00\end{cases} \quad (4)$$

The battery capacity of large EVs varies by the automaker. The following information in Table 1 pertains to EV battery capacities in typical EVs in Indonesia. Hence, the following setting for EV_{AR}^{U} in Eq. 3 and EV_{BC}^{U} in Eq. 4 is based on our data observation of the Indonesia EV market share, which includes customization and justification made for research intention and the context of an economic and environmental urban area in Jakarta and its neighboring cities.

2.3 Charger uncertainties

Charger uncertainties (CU) consider charging devices such as the power charge rating CH_{PR}^{U} and its efficiency and performance CH_{EP}^{U}. Similar to the EV uncertainty, CH_{PR}^{U} is taken from the charger perspective. In this research study, it is assumed that each plug rating of EVCS represents linearly. The lists of several EVCS in Indonesia and their specification in Table 2 are good references to justify setting values for charger uncertainties. The CU is derived using the following criteria in Eq. 5 and Eq. 6.

Table 2. Charger types and their charge rating (2020-2021)

EV type	Charger type	Power charge rating (kW$_{AC}$ | 3ϕ)	Quantity
4-Ws	AC type-2	22	40
	AC type-2	43	3
	AC type-2	33	2
	AC type-2	65	1
	AC type-2	20	22
	AC type-2	32	13
	AC type-1	10	11
	CCS-2	20	10
	AC	22	24
2-Ws	AC	1.44	2
	AC	< 5	7000

$$CH_{PR}^{U}(2|4\,Ws)\begin{cases}\xrightarrow{set\ (2\ \mathrm{Ws})} 2.2\ \mathrm{kW} \le CH_{PR}^{U} \le 5.5\ \mathrm{kW} \\ \xrightarrow{set\ (4\ \mathrm{Ws})} 12\ \mathrm{kW} \le CH_{PR}^{U} \le 43\ \mathrm{kW} \\ \text{s.t.} \\ \xrightarrow{when} T_{ON}^{Plug} \xrightarrow{If} Rand(T) = 1 \xrightarrow{then} \\ CH_{PR}^{U}(1) = (\rightarrow set\ (2|4\ \mathrm{Ws}) * CH_{EP}^{U}) \\ \xrightarrow{when} T_{OFF}^{Plug} \xrightarrow{If} Rand(T) = 0 \xrightarrow{then} \\ CH_{PR}^{U}(0) = 0.00\end{cases} \quad (5)$$

$$CH_{EP}^{U}(2|4\,Ws)\begin{cases}\xrightarrow{set\ (2\ \mathrm{Ws})} 0.85 \le CH_{EP}^{U} \le 0.92 \\ \xrightarrow{set\ (4\ \mathrm{Ws})} 0.90 \le CH_{EP}^{U} \le 0.93 \\ \text{s.t.} \\ \xrightarrow{when} T_{ON}^{Plug} \xrightarrow{If} Rand(T) = 1 \xrightarrow{then} \\ CH_{EP}^{U}(1) = (\rightarrow set\ (2|4\ \mathrm{Ws})) \\ \xrightarrow{when} T_{OFF}^{Plug} \xrightarrow{If} Rand(T) = 0 \xrightarrow{then} \\ CH_{EP}^{U}(0) = 0.00\end{cases} \quad (6)$$

Further, charger performance and efficiency are the scales of how efficiently the charger works, affecting how much current flows to the battery supplied from the AC grid. Notably, Tesla's charger is more efficient at 90% when using a fast charger and 99% by using a supercharger[27]. Moreover, the initial battery of its SoC also affects the charger efficiency due to the constant current (CC) session would take longer; by other means that a battery with a low SoC (by the time of initiating the charging session) has a higher value of efficiency than the one with a high SoC. Also, the environment's temperature affects how efficiently a charger operates. Additionally, it is found that the ideal temperature for charging/discharging is around +10°C (degree Celsius) to +30°C[28]. Notably, the fast charger's power conversion efficiency is 39% at -25°C and 93% at +25°C. Another acknowledged reference is that the most power conversion could only be reached 92% to 93% at maximum[28].

2.4 Estimated charging duration, power intake, and electrical energy

This part explains the predicted outputs derived from the abovementioned multi-uncertainties into three outputs parameters that can be used to justify their impact from the perspective of grid adequacy and security beforehand. The first parameter is estimated charging duration (ECD), as seen in Eq. 7, which calculates the time duration of charging adopted from[29]. Secondly, the estimated power intake (EPI) in Eq. 8 which calculates the summation of the delivered power in each plug's output. The third is the estimated energy usage (EEU) in Eq. 9 which calculates the accumulative energy absorbed from each EVCS. The overall estimated parameters are in an ideal condition ignoring the uncertainty assertion as seen in the following Eq. 7-9.

$$ECD = \frac{C_{EVbattery}^{Rat} \times (1 - SoC_{EVbattery}^{Rat}) \times DoD}{\eta_{charger} \times P_{EVCS}^{rat}} \tag{7}$$

$$EPI = \sum_{k=1}^{n} P_{EVCS,n}^{PRat} \tag{8}$$

$$EEU = ECD \times EPI \tag{9}$$

Where $C_{EVbattery}^{Rat}$ is EV's battery capacity (kWh), P_{EVCS}^{rat} is the power rating of EVCS (kW), n is the number of plugs in one charging station, and $P_{plug3,EVCS}^{PRat}$ is the power rating delivered by each plug (kW). The EPI per plug is $\sqrt{3} \times V_{L-L}^{Rat} \times I_{Ch}^{Rat} \times PF$, with the line-to-line voltage rating of the existing grid (V_{L-L}^{Rat}), the current charging rating of EVCS (I_{Ch}^{Rat}) and power factor (PF).

In contrast, those estimated parameters have been modified to include uncertainty factors determining the same parameters (ECD, EPI, and EEU), reflecting the multi-uncertainties randomness of the research objectives. Since the uncertainty parameters have different characteristics, as seen in Eq. 1-6, then the formula in Eq. 10-12 distinguishes different from the ideal conditions in Eq. 7-9 for the following.

$$ECD_{EV}^{U} = \frac{EV_{BC}^{U} \times (1 - UB_{SoC}^{U}) \times (EV_{BC}^{U} \times DoD^{U})}{CH_{EP(\%)}^{U} \times [CH_{PR}^{U} \times EV_{AR}^{U}]} \tag{10}$$

$$EPI_{EVCS}^{U} = \sum_{k=1}^{n} \left[\left(CH_{PR,n}^{U} \times EV_{AR}^{U} \right) + \left(CH_{PR,n}^{U} \times (1 - CH_{EP}^{U}) \right) \right] \tag{11}$$

$$EEU_{EVCS}^{U} = ECD_{EV}^{U} \times EPI_{EVCS}^{U} \tag{12}$$

2.5 Power system analysis (PSA) through load flow calculation

Power systems are constructed as a network of buses (nodes) and branches (lines). A network bus represents system parts, such as generators, loads, and substations. There are three different kinds of network buses. Depending on the type of buses, two of four quantities are primarily specified as a basis. The first is the slack or swing bus, where the known parameters are the voltage magnitude $|V_i|$ and the voltage phase angle (δ_i). Secondly, the generator bus or PV bus, where the known parameters are the active power (P_i) and $|V_i|$. Lastly, the load bus or PQ bus, where the known parameters are (P_i) and the reactive power (Q_i). The power flow problem or the load flow problem is the problem of figuring out the voltage magnitude $|V_i|$ and angle (δ_i) in each power system bus where the power generation and consumption are declared. By using Kirchhoff's Current Law (KCL) to describe the relationship between injected current $(\boldsymbol{I})$, and bus voltage $(\boldsymbol{V})$, in the form of the admittance matrix $(\boldsymbol{Y})$, whether the given system may be in single-phase, two-phase, or three-phase.

Aligning to the current discussion topic, let us assume the system is designed in three-phase *R, S,* and *T;* then the relationship can be described in the form of $\boldsymbol{Y}$ as follows as referenced from[30)-31)]:

$$I = \boldsymbol{YV} \leftrightarrow \begin{bmatrix} I_1^{RST} \\ \vdots \\ I_N^{RST} \end{bmatrix} = \begin{bmatrix} Y_{11}^{RST} & \cdots & Y_{1N}^{RST} \\ \vdots & \ddots & \vdots \\ Y_{11}^{RST} & \cdots & Y_{NN}^{RST} \end{bmatrix} \begin{bmatrix} V_1^{RST} \\ \vdots \\ V_N^{RST} \end{bmatrix} \tag{13}$$

To decompose each parameter in Eq. 13, then the given parameters of I_i^{RST}, V_i^{RST} and Y_i^{RST} are comprised as Eq. 14 below:

$$I_i^{RST} = \begin{bmatrix} I_i^R \\ I_i^S \\ I_i^T \end{bmatrix}, \; V_i^{RST} = \begin{bmatrix} V_i^R \\ V_i^S \\ V_i^T \end{bmatrix},$$

$$Y_{ij}^{RST} = \begin{bmatrix} Y_{ij}^{RR} & Y_{ij}^{RS} & Y_{ij}^{RT} \\ Y_{ij}^{SR} & Y_{ij}^{SS} & Y_{ij}^{ST} \\ Y_{ij}^{TR} & Y_{ij}^{TS} & Y_{ij}^{TT} \end{bmatrix} \tag{14}$$

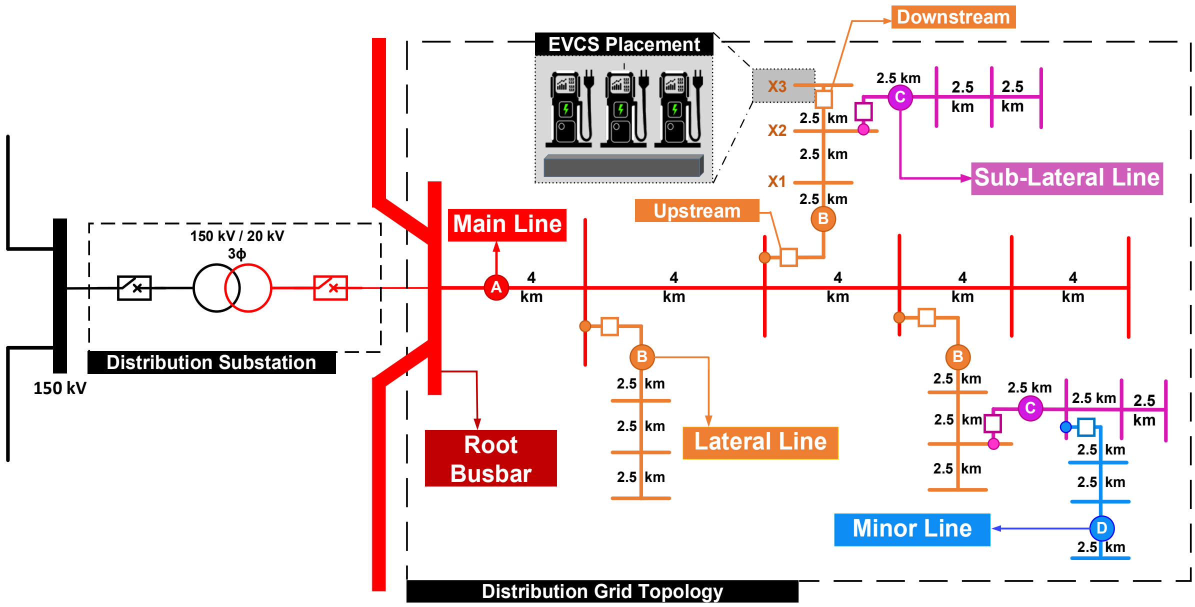

Fig. 2: Single line diagram (SLD) of typical distribution system feeder with the EVCS placement installation

where I_i^{RST} is the injected complex current, V_i^{RST} is the complex voltage at bus i (and in any total number of bus N), for a given phase-RST and Y_i^{RST} is the element of the admittance matrix. Then, also the injected current from the same equation can be computed at any given phase-RST as follows:

$$I_i^{RST} = \sum\nolimits_{k=1}^{N} . \sum\nolimits_{q=R|S|T} Y_{ik}^{RST|q} . V_k^q \quad (15)$$

The power flow problem of three-phase is given in the following mathematical Eq. 16:

$$S_i^{RST} = V_i^{RST} . \left(I_i^{RST}\right)^* =$$

$$V_i^{RST} . \sum\nolimits_{k=1}^{N} . \sum\nolimits_{q=R|S|T} \left(Y_{ik}^{RST|q}\right)^* . \left(V_k^q\right)^* \quad (16)$$

where S_i^{RST} is the injected complex power at bus i and $(I_i^{RST})^*$ is the complex conjugate form of the injected current. Generally, to mathematically solve the power flow problem is finding a solution to a nonlinear system of equations in which all variables are expressed as complex numbers. The S_i^{RST} is generally available in the form of three-phase unbalanced loads, to were distributed in all available buses of DGF in the form of $SL_i^{RST} = PL_i^{RST} + jQL_i^{RST}$. Hence, the PL_i^{RST} of each bus is derived from regular customer load and multi-uncertainty problems, as discussed. Afterwards, the PSA based on Newton-Raphson (NR) method[34] is used for load flow calculation to assess the behavior of the power system under different scenarios, which is to be validated using the typical DGF.

3. Case study

PSA is used to determine and analyze the behavior of existing power systems used as a validation framework, in which the power intake from 2|4-Ws EVCSs are tied in a typical 20 kV|0.4 kV DGF. The proposed DGF, as depicted in Fig. 2, is adopted from[34] and has been modified to reflect typical Indonesian DGF. Further, the allocated four units of 2|4-Ws EVCS are connected through a lateral line of medium voltage (MV) via a two-winding transformer of 250 kVA. The overall grid assets are referenced in the Indonesian standardized[35]. The line conductors for medium voltage (MV) are used as follows NFA2XSY-T 3x300+50, NFA2XSY-T 3x240+50, NFA2XSY-T 3x195+50, NFA2XSY-T 3x150+50, and NFA2XSY-T 3x120+50. Similarly, low voltage (LV) is used as follows NFA2X-T 3x150rm+95, NFA2X-T 3x120rm+95, NFA2X-T 3x95rm+95, and NFA2X-T 3x70rm+70. The regular load (non-EV demand) is measured from the actual distribution feeder in the east region of Jakarta within 24 hours in minutes of time-series data and be used as a base scenario loading profile for the research, as referenced in[36,37]. In order to maintain the research objectives, each distribution transformer is set to have a minimum loading of 33%–35% and a maximum loading of 65%–68%, which then arbitrarily determines each feeder's loading.

Meanwhile, the EVCS specification used in this research study consists of three plugs in each EVCS unit within different power ratings in the alternating current (AC) charging mode, as listed in Table 3. Continuously, the MCSM derives the input of each plug as the main research objective. At the same time, chargers' conversion efficiency and power factors are also included creating diversity with others. To further validate the research hypothesis, the PSA is then carried out through time-varying load flow calculation under quasi-dynamic simulation modeling (QDSM) adopted in[32,33], and utilized under balanced conditions to stay within the topic. It is done after the overall model, as shown in Fig.1, has been virtually built on the computer-aided engineering (CAE) program of DIgSILENT PowerFactory, which then be used to assess and validate the incoming related issues for future planning and operations of EVCS in the electrical power systems perspective.

Table 3. Two and four wheelers (2|4-Ws) charger specifications

Charger specs	2-Ws	4-Ws
$P_{[Plug-1]}$ Rating ($kW_{AC\,|\,3\phi}$)	≤ 2.0	≤ 12
$P_{[Plug-2]}$ Rating ($kW_{AC\,|\,3\phi}$)	≤ 3.9	≤ 22
$P_{[Plug-3]}$ Rating ($kW_{AC\,|\,3\phi}$)	≤ 5.3	≤ 43
$Efficiency_{(Min\text{-}Max)}$	0.85-0.92	0.90-0.93
Power factor (PF)	0.95	0.95

4. Results and discussion

This section discusses the MCSM results deriving the multi-uncertainties of charging behavior. Fig. 3 and 4 show the power derived from three plugs $P_{[Plug]}$ of each four of 2|4Ws EVCS. Two parameters that influenced the power drawn from each plug are the acceptable charge rating EV_{AR}^{U} of EV unit and the charger efficiency and performance CH_{EP}^{U}, which are arbitrarily generated, as referred to in Eq. 5 and Eq. 6 to the power plug charge rating CH_{PR}^{U} as a base reference. These sets of multi-uncertainties give an idea that the acceptable EV internal power conversion, its derivative parameter, and the charging efficiency value impact the power incurred per actuation.

Accordingly, the highest power incurred by the 4-Ws plug from slow, medium, and fast modes are plug-2 of the second unit, plug-2 of the fourth unit, and plug-3 of the third unit, of 13.506 kW, 23.945 kW, and 46.481 kW, respectively as shown in Fig.3 (a-d). The same result is that for the 2-Ws, it is found that the plug-1 of the first unit, plug-2 of the first unit, and plug-3 of the second unit, of 2.133 kW, 3.752 kW, and 5.792 kW, respectively, as shown in Fig.4 (a-d). While battery parameters (UB_{SoC}^{U}, DoD^{U}, EV_{BC}^{U}, $SoC_{EV}^{Set-OFF}$) and power parameters (EV_{AR}^{U}, CH_{EP}^{U}, CH_{PR}^{U}) are also impacted in various charging durations of 4-Ws (as seen in Fig.3). Similarly, it

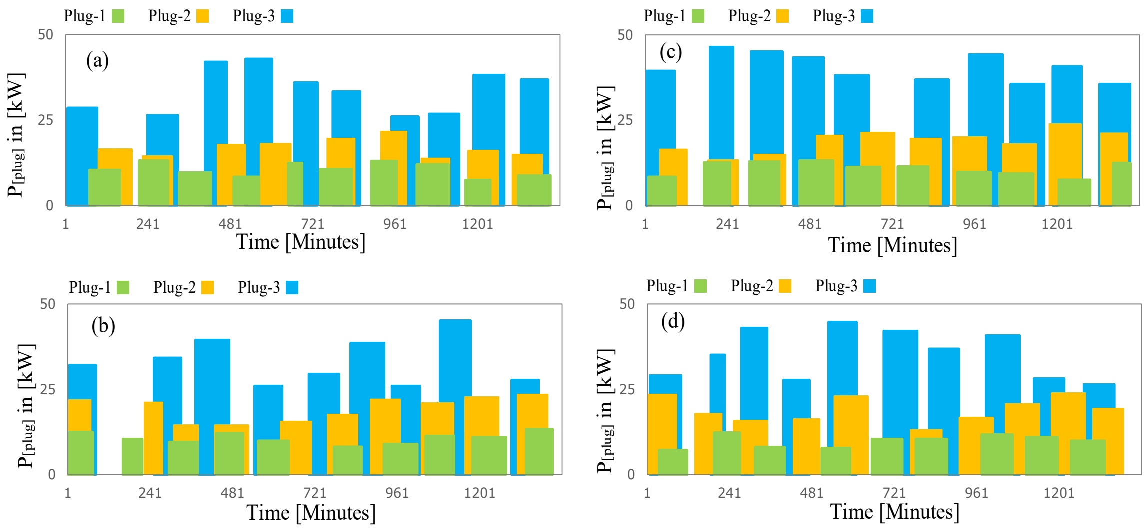

Fig. 3: Power incurred from each plug of unit A (a), unit B (b), unit C (c), and unit D (d) of 4-Ws EVCS after MCSM execution

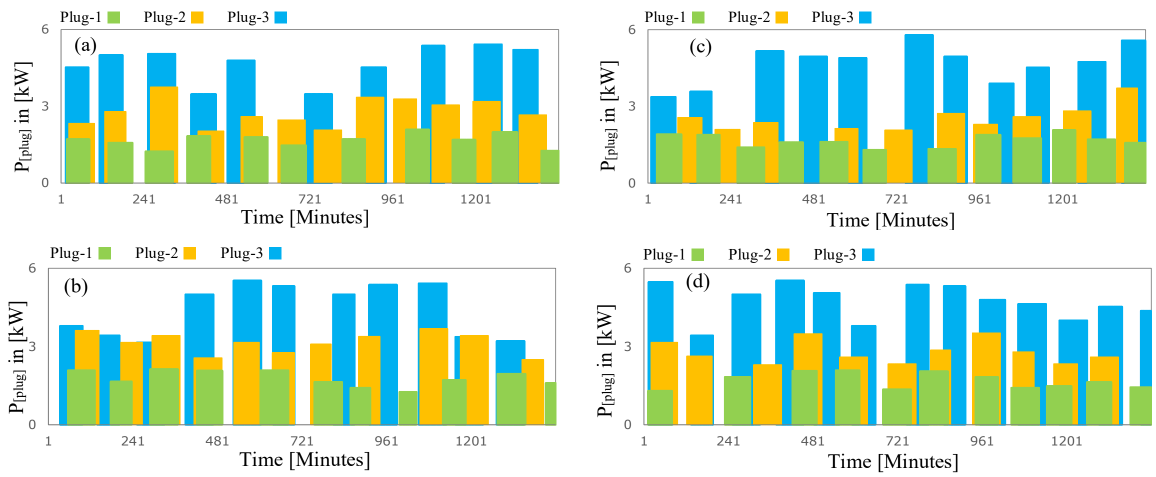

Fig. 4: Power incurred from each plug of unit A (a), unit B (b), unit C (c), and unit D (d) of 2-Ws EVCS after MCSM execution

happened as well for 2-Ws (as seen in Fig.4), which is further detailed in Table 4.

Admittedly, these high values of $P_{[Plug]}$ can be inferred that the EV unit could have the EV_{AR}^{U} almost equal to the range of CH_{PR}^{U} but then have low CH_{EP}^{U} which caused more power loss converted into thermal dissipation in reaching the rated value[27)]. In contrast, the brand-new EV unit could have a range close to of EV_{AR}^{U} (or even higher) that might have the power drawn almost equal to the plug charger rating CH_{PR}^{U} within maximum CH_{EP}^{U} (≈100%) during charging operation.

The rest of the results in Table 4 are intended to interpret how the multi-uncertainties randomness imposes the grid load profile related to high power intake, power charging duration per session, and the utilization of each plug (notably in Eq. 7-12), which then be relevant finding on how optioning the smooth transition in the pace of transformative urban transport sector and realignment mechanism to upscaling the supporting infrastructure in term of alerting the availability of financial support and finding effective strategies in tackling upcoming changes in the early stage adoption, especially for developing countries where private sector involvement has not exist yet due to economic low utilization[6,14)].

Table 4. Power incurred, time duration, and utilization of four units 2|4Ws EVCS

Characteristic	2-Ws plugs	4-Ws plugs
Power drawn		
Max. P_{plug1} (kW_{AC})	2.133	13.506
Min. P_{plug1} (kW_{AC})	1.244	7.253
Max. P_{plug2} (kW_{AC})	3.752	23.945
Min. P_{plug2} (kW_{AC})	2.040	13.203
Max. P_{plug3} (kW_{AC})	5.792	46.481
Min. P_{plug3} (kW_{AC})	3.159	26.064
Duration		
$ECD_{longest\text{-}active}$ (minutes)	80	100
$ECD_{shortest\text{-}active}$ (minutes)	29	43
$ECD_{longest\text{-}idle}$ (minutes)	164	167
$ECD_{shortest\text{-}idle}$ (minutes)	9	5
Utilization		
Max. $P_{plug\text{-}active}$ (times)	13	10
Min. $P_{plug\text{-}active}$ (times)	10	9
Max. $P_{plug\text{-}idle}$ (times)	13	11
Min. $P_{plug\text{-}idle}$ (times)	11	10
Max. $P_{plug\text{-}utilized}$ (%)	62.68	64.49
Min. $P_{plug\text{-}utilized}$ (%)	50.80	54.48
Max. $P_{plug\text{-}not\ utilized}$ (%)	49.17	45.56
Min. $P_{plug\text{-}not\ utilized}$ (%)	37.36	35.56

Finally, the validation through load flow computation from the affected multi-uncertainties factors that emerged from the charging process of public EVCS is discussed. The issues related to voltage stability are foremost assessed since it is one of the statutory parameters of the distribution grid's day-to-day operation, as depicted in Fig. 5 (a) and (b).

By viewing the DGF topology (see Fig. 2), the actuation of EVCS slightly influenced voltage magnitudes at X1 and X2 nodes of upstream MV nodes, which flow through the downstream X3 node and supply the EVCS demand via point of connection (PoC). The slight deviation of 0.001 p.u. in minimum voltage deviation ($V_{Min\text{-}Dev}$) starting from node X3 to node X1 (before and after EVCS actuation) is shown in Fig. 5(a). These changes may be subtle but can lead to important changes if more EVCS units are, i.e., featured with direct current (DC) charger units. Meanwhile, the most stranded V_{Mag} of 0.022 p.u. ($V_{Min\text{-}Dev}$ ≈ -2.2%) is encountered in the incoming LV node of its PoC. Furthermore, the stranded dip of 0.884 p.u. occurred due to plugging activation concurrently with the peak hour of regular non-EV load, as shown in Fig. 5(b), which put $V_{Min\text{-}Dev}$ at -11.59% out of -9.41% before integration. Hence, this finding suggests that more EVCS integration should be thoroughly assessed since it passed the voltage regulation of -10% under-voltage (UV) setup, which led to significant voltage stability issues along the feeder. Further, it indicates that the higher sensitivities in voltage magnitudes are due to the higher utilization factor of the transformer capacity in the LV grid than in MV[38)].

Other aspects of our research findings related to power intake, accumulative energy, and the grid loss (before-after) of the integration are depicted in Table 5, which can be used to foresee future challenges of e-mobility-supportive infrastructure and the rethinking strategy.

Table 5. Power and energy supplied and grid adequacy before and after integration of four units EVCS

Characteristic	Before integration	After integration
Power & energy supplied		
Max. Power $_{P\text{-}incurred}$ (kW_{AC})	n.a.	173.38
Min. Power $_{P\text{-}incurred}$ (kW_{AC})	n.a	95.53
Power Loss $_{Upstream}$ (kW_{AC})	31.97	32.10
Power Loss $_{Downstream}$ (kW_{AC})	25.19	25.82
Total Energy Operation (MWh) per-24h operation	n.a	2.292
Grid adequacy		
Max. $V_{\text{-}deviation}$ at PoC (%)	-6.07	-6.32
Min. $V_{\text{-}deviation}$ at PoC (%)	-9.41	-11.59
Max. $Trafo_{loading}$ per-24h (%)	0.21	78.2
Min. $Trafo_{loading}$ per-24h (%)	0.20	0.69
Max. $Line_{loading}$ upstream (%)	39.37	41.04
Min. $Line_{loading}$ upstream (%)	27.28	27.67
Max. $Line_{loading}$ downstream (%)	36.50	37.75
Min. $Line_{loading}$ downstream (%)	24.88	25.32

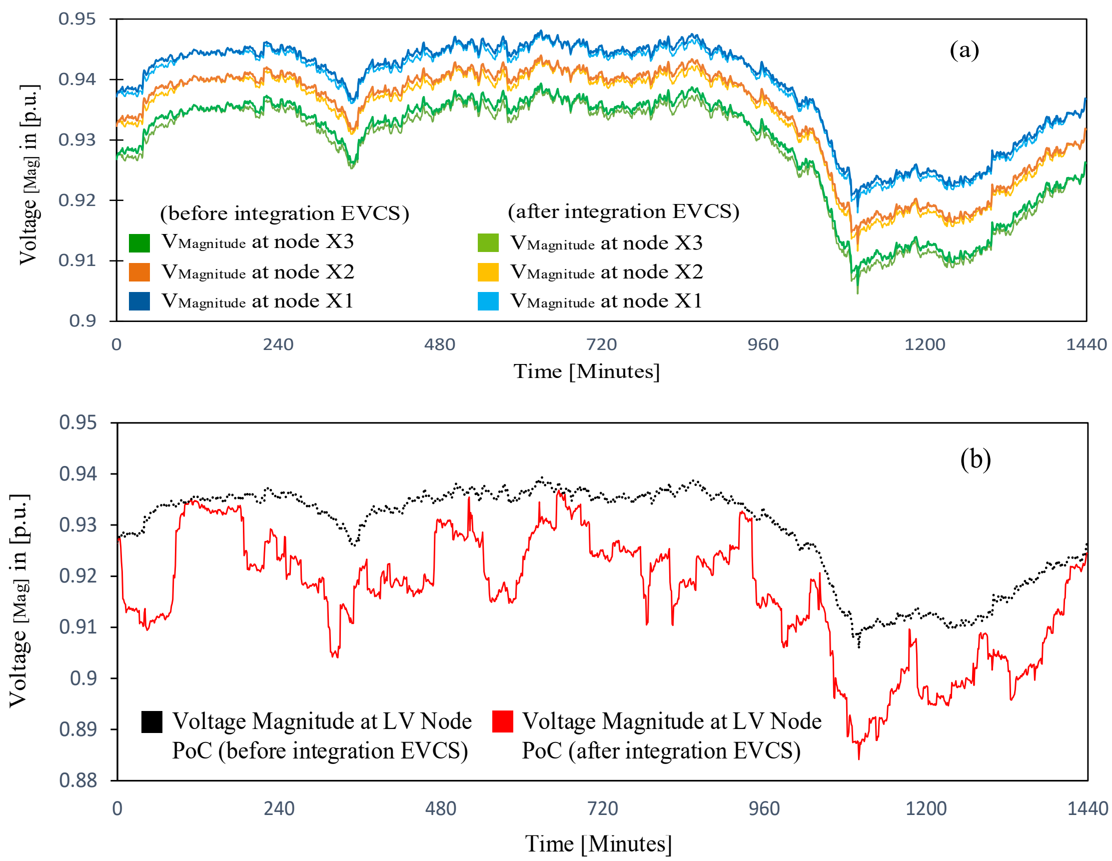

Fig. 5: Impact of multi-uncertainties against voltage magnitude at MV node PoC (a) and LV node PoC (b) before and after integration of four units 2|4-Ws EVCS

As can be seen in Table 5, these parameters are concerned with the grid's adequacy and capacity for future assessment and evaluation as intended by the current proposed framework. Other than that, since the existing DGF infrastructure and its asset's ability is mostly default given; therefore, seeking in-service grid capability and capacity (so-called hosting capacity, HC) is a tremendous challenge due to the inherent diversity and complexity of DGF. Therefore, the current result data (of time-varying execution framework model) provide preliminary power demand fluctuation, which could address and discover the behavior trends needed in conducting HC. Nevertheless, the simultaneous process (derived by incidental concurrences of plug actuation) operation reached power drawn at the highest of 173.38 kW, acquiring the transformer loading of 78.2%. In comparison, the transformer loading average is 43.1%, which leads to the loading factor being around 0.551. In contrast, low power utilization of 0.69% is due to the other internal apparatus supporting the operation, such as the lighting equipment and others, while the plugs are majority not in-used or idled.

5. Conclusions

The relevant findings contribute to developing a practical validation framework that should lead reasonably to the utility and grid operator for future planning and operation linked to grid infrastructure adequacy awareness and early-stage preparation in supporting the national commitment to energy transition through the future electrification transport (EE) program. Our current findings also estimate the plug's power usage of EVCS 2|4Ws with multi-uncertainties in urban-area, which have been elaborated in this research, consisting of user behavior, EV unit, and charger uncertainties. Our simulation results show that the maximum power drawn, duration, and charger utilization for 4-Ws plug are 46.48 kW, 100 minutes, and ten times daily. The voltage magnitude dropped 0.022 p.u. occurs in the MV node during the peak load, while it could reach 0.884 p.u in the LV node and, thus, violate under-voltage regulation, despite the transformer loading at 78.2%, and minimum loading is only 0.69%. In that scene, integrating EVCS has a more significant impact on the LV grid, with the voltage stability becoming more sensitive to the presence of EVCS.

The findings show that the framework model projection enables the stakeholders or operators to foresee, validate and justify their existing grid conditions' of its adequacy and security awareness, especially with the potential abrupt power incurred that could threaten the daily grid operational ability and alert them of what should be prioritized toward the gradual EE's planning program.

Finally, this study indicates that special attention should be given and a better understanding of how the multi-uncertainties randomness undoubtedly imposes on the grid conditions. Hence, future planning and reconfiguring to where the EVCS be placed and its coverage sizing and in-service quantity and capacity versus the influenced diversity factors (i.e., EV unit market shared, the occupational workplace and locations, and demographic coverage area in achieving better services and prevent future operational obstacles in the DGF infrastructure) is highly urged in the pace of e-mobility. Therefore, future research considering the practicable diversities mentioned above on how the EVCS placement is optimally supplied from different existing feeders, including combined AC and DC plugs and feeder HC optimization, while still using the substantial current findings method to derive the multi-uncertainties for specific regions, i.e., city or province scope remains unaddressed and still relevant to insight the stakeholders. Above all, addressing (by minimizing or avoiding) future operational congestion within fairly grid upgrading cost (if necessary) align with gradual planning of ICE to EV substitution is still open, fulfilling the national energy transition agenda.

Acknowledgements

This research has been carried out as part of mandatory tasks of the intelligent power energy system (InPES) research group and its members in the research center for energy conversion and conservation (PRKKE), a research organization of energy & manufacture (OREM) of national research & innovation agency (BRIN). The authors thank the reviewers and editor for their valuable comments and suggestions.

Nomenclature

Upstream	The interconnection between the main MV line through the first MV (node X1) of the sub-lateral line
Downstream	The interconnection between the sub-lateral line until the MV nodes where EVCS tied in (node X3)
DGF	distribution grid feeder
DoD	depth of discharge
ECD	estimated charging duration (hour)
EEU	estimated energy usage (kWh)
EV	electric vehicle
EPI	estimated power intake (kW)
EVCS	electric vehicle charging station
ICE	internal combustion engine
MCSM	monte-carlo simulation method
PSA	power system analysis
SoC	state of charge (%)
V_{Mag}	voltage magnitude (p.u.)
$V_{\mathrm{Min\text{-}Dev}}$	voltage minimum deviation (%)
$C_{battery}$	battery capacity (kWh)
χ^{U}	uncertainty of any entities
UU	user behavior uncertainty on willingness to utilize the SoC of battery capacity
UB^{U}_{SoC}	user behavior uncertainty on willingness to utilize the SoC of battery capacity
$UB^{U}_{S\|S}$	user behavior uncertainty on willingness to start or stop the charging process ignoring the SoC battery state
EV^{U}_{AR}	electric vehicle uncertainty on acceptable charge rating (kW)
EV^{U}_{BC}	electric vehicle uncertainty on battery capacity (kWh)
CH^{U}_{EP}	charger uncertainty on charger's efficiency and performance (%)
CH^{U}_{PR}	charger uncertainty on power charge rating (kW)
$T^{Plug}_{On\|Off}$	the time of active plug and the idle time of charging
$HO^{\,active}_{\,EVCS}$	total hour of EVCS operation (minutes|hours)
$T^{Set-ON\|OFF}_{EVCS}$	time set (On) or set (Off) of EVCS operation (hh:mm)
$SoC^{\,Set-ON}_{\,EV}$, $SoC^{\,Set-OFF}_{\,EV}$	limitation percentage of SoC at the beginning of charging (on) and the stoppage SoC limit (off) (%)
$SoC^{\,Rat}_{\,EV}$	the SoC rating of EV unit taken factory per as-built
$\mathrm{Plug}^{\mathrm{PRat}}_{\mathrm{EVCS}}$	power plug rating of EVCS (kW)
$P_{plug}{}^{\mathrm{Rat}}_{\mathrm{EVCS}}$	power plug incurred during EVCS operation (kW)
SL^{RST}_{i}	apparent power load at three-phase of R|S|T in bus i (VA)
PL^{RST}_{i}	active power load at three-phase of $^{R\|S\|T}$ in bus i (W)
jQL^{RST}_{i}	reactive power load at three-phase of $^{R\|S\|T}$ in bus i in imaginary form (VAR)
V^{RST}_{i}	voltage at a given of three-phase of $^{R\|S\|T}$ at bus i (volt)
I^{RST}_{i}	the injected current at a given of three-phase of $^{R\|S\|T}$ at bus i (A)

References

1) Abdelgader A.S. Gheidan, Mazlan Bin Abdul Wahid, Opia A. Chukwunonso, and Mohd Fairus Yasin,

"Impact of internal combustion engine on energy supplyand its emission reduction via sustainable fuel source," Evergreen, 9(3) 830–844 (2022). doi:10.5109/4843114.

2) Muhammad Idham Sabtu, Hawa Hishamuddin, N. Saibani, and Mohd Nizam Ab Rahman, "A review of environmental assessment and carbon management for integrated supply chain models," Evergreen, 8(3) 628–641 (2021). doi:10.5109/4491655.
3) Nurul Syafiqah Zulkefly, H. Hishamuddin, Fatin Amrina A. Rashid, N. Razali, N. Saibani, and Mohd Nizam Ab Rahman, "The effect of transportation disruptions on cold chain sustainability," Evergreen, 8(2) 262–270 (2021). doi:10.5109/4480702.
4) A. Habibie, M. Hisjam, W. Sutopo, and M. Nizam, "Sustainability evaluation of internal combustion engine motorcycle to electric motorcycle conversion," Evergreen, 8(2) 469–476 (2021). doi:10.5109/4480731.
5) S. Sawant, Raja Mazuir Raja Ahsan Shah, M. Rahman, Abd Rashid Abd Aziz, S. Smith, and A. Jumahat, "System modelling of an electric two-wheeled vehicle for energy management optimization study," Evergreen, 8(3) 642–650 (2021). doi:10.5109/4491656.
6) "Global ev outlook 2022 - securing supplies for an electric future," (2022). https://iea.blob.core.windows.net/assets/ad8fb04c-4f75-42fc-973a-6e54c8a4449a/GlobalElectricVehicleOutlook2022.pdf (accessed August 8, 2022).
7) "Governor newsom announces california will phase out gasoline-powered cars & drastically reduce demand for fossil fuel in california's fight against climate change," CAWeb Publishing Service, (2020). https://www.gov.ca.gov/2020/09/23/governor-newsom-announces-california-will-phase-out-gasoline-powered-cars-drastically-reduce-demand-for-fossil-fuel-in-californias-fight-against-climate-change/ (accessed August 30, 2022).
8) Steve Scherer, "Canada to ban sale of new fuel-powered cars and light trucks from 2035," Reuters.Com, (2021). https://www.reuters.com/world/americas/canada-ban-sale-new-fuel-powered-cars-light-trucks-2035-2021-06-29/ (accessed August 8, 2022).
9) "Mission zero - powered by holland," (2019). https://www.rvo.nl/sites/default/files/2019/06/Mission%20Zero%20Powered%20by%20Holland.pdf (accessed August 8, 2022).
10) "Earth day 2021 arrives as u.s. electric vehicle sales continue to grow," (2021). https://www.bts.gov/data-spotlight/electric-vehicle-use-grows (accessed August 8, 2022).
11) "The state of ev charging infrastructure in europe by 2030," (2022). https://www.virta.global/blog/ev-charging-infrastructure-development-statistics (accessed August 8, 2022).
12) "E-mobility in thailand," (2021). https://www.rvo.nl/sites/default/files/2021/10/E-Mobility%20in%20Thailand.pdf (accessed August 8, 2022).
13) A. Pribadi, "PLN engages private sector to install more charging stations," (2022). https://www.esdm.go.id/en/media-center/news-archives/pln-gandeng-pihak-swasta-perbanyak-spklu-dengan-skema-bagi-hasil (accessed September 11, 2022).
14) M.O. Metais, O. Jouini, Y. Perez, J. Berrada, and E. Suomalainen, "Too much or not enough? planning electric vehicle charging infrastructure: a review of modeling options," Renewable and Sustainable Energy Reviews, 153 111719 (2022). doi:10.1016/j.rser.2021.111719.
15) U.H. Ramadhani, "Uncertainty and correlation modeling for load flow analysis of future electricity distribution systems: Probabilistic modeling of low voltage networks with residential photovoltaic generation and electric vehicle charging," UPPSALA UNIVERSITET, n.d. urn:nbn:se:uu:diva-434951 (accessed July 10, 2022).
16) C.B. Jones, M. Lave, W. Vining, and B.M. Garcia, "Uncontrolled electric vehicle charging impacts on distribution electric power systems with primarily residential, commercial or industrial loads," Energies, 14 (6) 1688 (2021). doi:10.3390/en14061688.
17) M.A. Awadallah, B.N. Singh, and B. Venkatesh, "Impact of ev charger load on distribution network capacity: a case study in toronto," Can. J. Electr. Comput. Eng., 39 (4) 268–273 (2016). doi:10.1109/CJECE.2016.2545925.
18) K.N. Hasan, K.M. Muttaqi, P. Borboa, J. Scira, Z. Zhang, and M. Leishman, "Measurement-based Electric Vehicle Load Profile and Its Impact on Power System Operation," in: 2019 9th International Conference on Power and Energy Systems (ICPES), IEEE, Perth, WA, Australia, 2019: pp. 1–6. doi:10.1109/ICPES47639.2019.9105651.
19) M. Motinur Rahman, S. Saha, M. Z. H. Majumder, T. Tamrin Suki, M. Habibur Rahman, F. Akter, M. A. S. Haque, and M. Khalid Hossain, "Energy conservation of smart grid system using voltage reduction technique and its challenges," Evergreen, 9(4) 924–938 (2022). doi:10.5109/6622879.
20) A. Almaghrebi, X. Cheng, K. James, and M. Alahmad, "Analysis of PEV User Charging Behavior at Household Charging Stations, Omaha Case Study," in: 2021 IEEE Transportation Electrification Conference & Expo (ITEC), IEEE, Chicago, IL, USA, 2021: pp. 561–566. doi:10.1109/ITEC51675.2021.9490079.
21) "Integrated statistical services, central bureau of statistics 2022," (n.d.). https://pst.bps.go.id/ (accessed September 1, 2022).
22) "Economic and business statistics data portal, katadata indonesia 2022," (n.d.).

https://databoks.katadata.co.id/ (accessed July 25, 2022).
23) P.D. Coddington, "ANALYSIS of random number generators using monte carlo simulation," Int. J. Mod. Phys. C, 05 (03) 547–560 (1994). doi:10.1142/S0129183194000726.
24) M. Kane, "Tesla: battery capacity retention averages 90% after 200,000 miles," INSIDEEVs, (2021). https://insideevs.com/news/525820/tesla-battery-capacity-retention-90/ (accessed September 11, 2022).
25) T. Moloughney, "What are the different levels of electric vehicle charging?," Forbes.Com, (n.d.). https://www.forbes.com/wheels/advice/ev-charging-levels/ (accessed September 9, 2022).
26) M. Corno, and G. Pozzato, "Active adaptive battery aging management for electric vehicles," IEEE Trans. Veh. Technol., 69 (1) 258–269 (2020). doi:10.1109/TVT.2019.2940033.
27) John Voelcker, "EVs explained: charging losses," (2021). https://www.caranddriver.com/features/a36062942/evs-explained-charging-losses/ (accessed September 2, 2022).
28) G. Trentadue, A. Lucas, M. Otura, K. Pliakostathis, M. Zanni, and H. Scholz, "Evaluation of fast charging efficiency under extreme temperatures," Energies, 11 (8) 1937 (2018). doi:10.3390/en11081937.
29) M. Lei, and M. Mohammadi, "Hybrid machine learning based energy policy and management in the renewable-based microgrids considering hybrid electric vehicle charging demand," International Journal of Electrical Power & Energy Systems, 128 106702 (2021). doi:10.1016/j.ijepes.2020.106702.
30) J. B. V. Subrahmanyam, and C. Radhakrishna, "A simple approach of three phase distribution system modeling for power flow calculations," (2010). doi:10.5281/ZENODO.1085954.
31) B. Sereeter, K. Vuik, and C. Witteveen, "Newton power flow methods for unbalanced three-phase distribution networks," Energies, 10 (10) 1658 (2017). doi:10.3390/en10101658.
32) "DIgSILENT GmbH, 'Load Flow Analysis' in User Manual DIgSILENT PowerFactory: Chapter 25, (DIgSILENT GmbH, Gomaringen, 2020), ch.25," in: n.d.: pp. 420–428.
33) "DIgSILENT GmbH, 'Quasi-Dynamic Simulation' in User Manual DIgSILENT PowerFactory: Chapter 28, (DIgSILENT GmbH, Gomaringen, 2020), ch.28," in: n.d.: pp. 528–533.
34) K. Vinoth Kumar, and M.P. Selvan, "A simplified approach for load flow analysis of radial distribution network with embedded generation," in: TENCON 2008 - 2008 IEEE Region 10 Conference, IEEE, Hyderabad, India, 2008: pp. 1–6. doi:10.1109/TENCON.2008.4766843.
35) "Working Standard Group for the Distribution of Electricity Network and the University of Indonesia Science and Technology Research Center, Book 1: Criteria for Electric Power Distribution Network Construction Engineering (PT PLN (PERSERO), 2010)," in: n.d.: pp. 3–7, 23–28.
36) A.W. Syamroni, and A.A. Basharah, "Time series measurement data of medium voltage | low voltage [mv|lv] feeders in jabodetabek regions indonesia – district incoming transformers of 630 kva & 400 kva (20 kv | 0.4 kv)," (2022). doi:10.5281/ZENODO.7954007.
37) A.W. Syamroni, and A.A. Basharah, "Time series measurement data of office building in jakarta indonesia - incoming transformer of 20 kv | 0.4 kv," (2022). doi:10.5281/ZENODO.7953940.
38) W.H. Kersting, "Distribution system modeling and analysis," Fourth edition, CRC Press, Boca Raton, FL, 2018.